Biointerface Research in Applied Chemistry
Open-Access Journal (ISSN: 2069-5837)

Article
Volume 13, Issue 3, 2023, 299
https://doi.org/10.33263/BRIAC133.299

Synthesis, *In silico* Molecular Docking Studies and antimicrobial evaluation of Some New Anthracene Derivatives Tagged with Arylidene, Pyridine, Oxazole, and Chromene Moieties as Promising Inhibitors of Bacterial DNA gyrase

Hemat M. Dardeer [1], Ahmed G. Taha [1], Arafat Toghan [1,2,*], Aboubakr H. Abdelmonsef [1]

[1] Chemistry Department, Faculty of Science, South Valley University, Qena 83523, Egypt; prof_hemat@yahool.com (H. M. D.); ahmad.gaber@svu.edu.eg (A.G.T.); arafat.toghan@yahoo.com (A.T.); aboubakr.ahmed@sci.svu.edu.eg (A.H.A.);
[2] Chemistry Department, College of Science, Imam Mohammad Ibn Saud Islamic University (IMSIU), Riyadh 11623, Saudi Arabia; arafat.toghan@yahoo.com (A.T.);
* Correspondence: arafat.toghan@yahoo.com (A. Toghan);

Scopus Author ID 36437624000
Received: 2.04.2022; Accepted: 16.05.2022; Published: 19.07.2022

Abstract: Here, A series of unprecedented derivatives of several heterocyclic compounds, including arylidene, pyridine, oxazole, and chromene, were designed with the anthracene moiety starting from 2-cyano-pyrroloanthracen acetamide (1). The chemical composition of all synthesized compounds was established by spectral analysis FT-IR, ^{1}H-NMR, ^{13}C-NMR, and Mass spectra. Also, the new compounds were docked to the active site of the DNA gyrase B chain enzyme, and the suitable binding interactions were displayed according to their bond lengths and conformational energies. The structure-activity relationship analysis showed that the antimicrobial activity could be modulated by the existence of anthracene moiety, electron-withdrawing groups, and amide linkage. *In silico* ADMET (absorption, metabolic, distribution, toxicity, and excretion) predictions for the compounds 1-7 were calculated to gain insight into their pharmacokinetics, safety, and drug-likeness profile. The antimicrobial investigations of all synthesized molecules were achieved against Gram-negative (*Escherichia coli*) and Gram-positive (*Bacillus cereus*) bacterial strains. Results indicated that the compounds exhibited promising activity against strains. Therefore, the newly hybrid anthracene molecules could serve as promising chemical scaffolds to develop upcoming drug candidates as antimicrobial agents.

Keywords: anthracene; arylidene; chromene; DNA gyrase B chain enzyme; docking study; antimicrobial agents.

1. Introduction

Pyridines and isoxazoles are important heterocyclic scaffolds in the fields of medicine, pharmacology, agriculture, materials, and several industries [1]. The literature survey revealed that many pyridine and isoxazole derivatives have been used for pharmacological applications, such as anticonvulsant [2], cytostatic [3], antihistaminic agents [4], muscarinic agonists for the treatment of Alzheimer's disease [5], rotaxanes [6], chemiluminescent [7], nucleosides [8], antifungal [9], antioxidant [10], antimicrobial [11], antinociceptive [12], anti-inflammatory [13], HDAC inhibitory [14], analgesic [15], antitumor [16], nematicidal [17], anticancer [18], antiviral [19], antituberculosis [20], antimycobacterial [21], hypoglycemic, and

immunosuppressive [22]. Pyridine-derived pharmaceuticals include atazanavir [23] and imatinib mesylate in the last few decades. These drugs are dubbed for human immunodeficiency virus (HIV) and chronic myelogenous leukemia. It was reported that pyridine derivatives are also incorporated into polymers such as polyvinyl pyridine [24]. For over a century, chemists have developed methodologies for synthesizing pyridine derivatives, and it is unlikely that interest in the field will decrease due to the continued importance of the pyridine core in both biological and chemical fields. Previous studies have reported that heterocyclic compounds such as pyridines and chromenes derivatives containing anthracene skeleton had antimicrobial activity against *E. coli* [25], as represented in Figure 1.

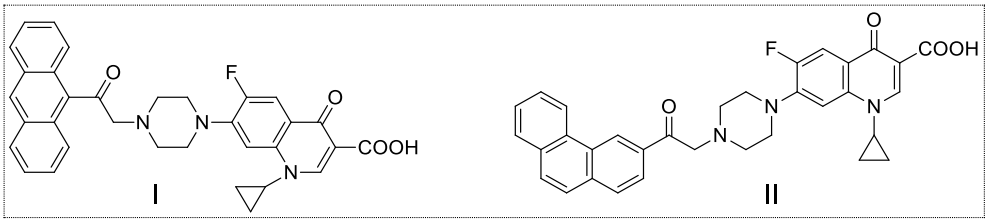

Figure 1. Examples of antimicrobial agents containing anthracene moiety.

Despite the technological and scientific progress in facing infectious and epidemic diseases caused by the spread of many microbes, using appropriate antibiotics, their residues remain a pollutant for the environment and society. DNA gyrase B is an important bacterial enzyme involved in controlling the topological transition of DNA [26]. The inhibition of this enzyme is responsible for the distribution of DNA synthesis and cell death [26]. Therefore, it has been selected as a therapeutic target for identifying and developing antimicrobial agents.

In our effort to develop new, potent, and less toxic antimicrobial candidates, a novel series of anthracene analogs coupled to five or six hetero membered rings were synthesized. Furthermore, computer-aided drug screening by docking studies and ADMET analysis was accomplished for the compounds **1-7**, to explore their mode of action versus the target enzyme DNA gyrase B chain. The completion of the present work indicated that the compounds were successfully docked to the target protein with good docking scores ranging from -11.3 to -8.4 kcal/mol.

2. Experimental

2.1. Materials and instruments.

All reagents used were of analytical grade. Melting points were evaluated on a Buchi apparatus and are uncorrected, IR spectra, KBr pellets, 500–4000 cm^{-1} were recorded on a Thermo Nicolet NEXUS 670 FT-IR spectrophotometer, with 0.125 cm^{-1} spectral resolution. ^{1}H-NMR spectra were measured on a Bruker AM 400 instrument. Chemical shifts are expressed as values relative to TMS as an internal standard. Multiplicities are designated as singlet (s), doublet (d), triplet (t), quadruplet (q), and multiplet (m).

2.2. General procedure for the preparation of the anthracene derivatives.

Equimolar ratio mixture (0.001 mol) of (1) and corresponding reactant in ethanol (10 mL) as a solvent and TEA (0.01 mL) were heated for the proper time, gave white powder, filtered, and purified from ethanol to give anthracene derivatives as white crystals.

2.2.1. (11S,15R)-13-((5-aminoisoxazol-3-yl)amino)-10,11-dihydro-9H-9,10-[3,4]epipyrroloanthracene-12,14(13H,15H)-dione (2).

It was prepared according to the general procedure using 2-cyano-*N*-((11*S*,15*R*)-12,14-dioxo-11,12,14,15-tetrahydro-9*H*-9,10-[3,4]epipyrroloanthracen-13(10*H*)-yl)acetamide and hydroxylamine hydrochloride. The product was obtained after 6 hrs as white powder. Yield: 75 %, m. p.: 255-258 °C.FTIR (KBr): ν/cm^{-1}= 3345 (NH), 3010 (CH-aromatic), 1760, 1708 (C=O); ^{1}H-NMR (DMSOd$_6$) δ (ppm) = 3.17- 3.20 (d, d, 2H), 4.62 (s, NH), 4.77 (d, d, 2H), 7.12 (s, 1H), 7.12-7.46 (m, 8H, Ar-H); ^{13}C NMR (100 MHz, DMSO-d_6): δ 43.65, 44.69, 44.83, 44.98, 124.77, 125.24, 125.47, 127.15, 128.75, 129.51, 129.97, 130.94, 172.60, 174.35; MS (EI, 70 eV): m/z (%) = 374 (M$^+$, 30 %); Chemical formula: $C_{21}H_{18}N_4O_3$:(374.5); Calculated: C, 67.92; H, 4.58; N, 18.86; Found: C, 67.94; H , 4.60; N, 18.88.

2.2.2. (E)-3-(4-chlorophenyl)-2-cyano-N-((11S,15R)-12,14-dioxo-11,12,14,15-tetrahydro-9H-9,10-[3,4]epipyrroloanthracen-13(10H)-yl)acrylamide (3).

It was obtained according to the general procedure using 2-cyano-*N*-((11*S*,15*R*)-12,14-dioxo-11,12,14,15-tetrahydro-9*H*-9,10-[3,4]epipyrroloanthracen-13(10*H*)-yl)acetamide and 2-(4-chlorobenzylidene)malononitrile. The product was obtained after 15 hrs as white powder. Yield: 70 %, m. p.: 227-229 ºC. FTIR (KBr): ν/cm^{-1}= 3332 (NH), 3009 (CH-aromatic), 2205 (CN), 1785, 1720 (C=O); ^{1}H-NMR (DMSOd$_6$) δ (ppm) = 3.45 (d, d, 2H), 4.87 (d, d, 2H),7 .11-7.98 (m, 8H, Ar-H), 8.46 (s, 1H); ^{13}C NMR (100 MHz, DMSO-d_6): δ 44.49, 44.59, 44.89, 45.10, 45.35, 124.12, 125.60, 125.23, 125.60, 126.85, 127.19, 127.37, 129.65, 130.16, 130.39, 130.58, 131.73, 132.97, 137.48, 138.01, 139.05, 142.52, 169.77, 171.57, 173.95; MS (EI, 70 eV): m/z (%)= 479 (M+, 18 %); Chemical formula: $C_{28}H_{18}N_3O_3Cl$: (479.5); Calculated: C, 70.07; H, 3.54; N, 8.75, Cl,7.40; Found: C, 70.09; H, 3.55; N, 8.77, Cl, 7.38.

2.2.3. (E)-2-cyano-N-((11S,15R)-12,14-dioxo-11,12,14,15-tetrahydro-9H-9,10-[3,4]epipyrroloanthracen-13(10H)-yl)-3-phenylacrylamide (4).

It was prepared according to the general procedure using 2-cyano-*N*-((11*S*,15*R*)-12,14-dioxo-11,12,14,15-tetrahydro-9*H*-9,10-[3,4]epipyrroloanthracen-13 (10*H*)-yl)acetamide **(1)** and 2-benzylidenemalononitrile. The product was obtained after 18 hrs as white powder. Yield: 76 %, m. p.: 220-222 ºC. FTIR (KBr): ν/cm^{-1}= 3345 (NH), 3012 (CH-aromatic), 2207 (CN), 1770, 1730 (C=O); ^{1}H-NMR (DMSOd$_6$) δ (ppm) = 3.30-3.37 (d, d, 2H), 4.88 (d, d, 2H), 7.17-7.70 (m, 8H, Ar-H), 8.32 (s, 1H); ^{13}C NMR (100 MHz, DMSO-d_6): δ 44.37, 44.24, 45.47, 45.87,124.58, 125.13, 125.91, 126.77, 128.75, 129.51, 129.97, 130.82, 132.55, 134.04, 163.94, 169.67, 171.93, 173.83; MS (EI, 70 eV): m/z (%) = 444 (M$^+$, 24 %); Chemical formula: $C_{28}H_{18}N_3O_3$: (444.5); Calculated: C, 68.58; H, 3.46; N, 11.42; Found: C, 68.57; H, 3.48; N, 11.44.

2.2.4. 4-(4-chlorophenyl)-1-((11S,15R)-12,14-dioxo-11,12,14,15-tetrahydro-9H-9,10-[3,4]epipyrroloanthracen-13(10H)-yl)-6-hydroxy-2-oxo-1,2,3,4-tetrahydro pyridine-3,5-dicarbonitrile (5).

It was prepared according to the general procedure using 2-cyano-*N*-((11*S*,15*R*)-12,14-dioxo-11,12,14,15-tetrahydro-9*H*-9,10-[3,4]epipyrroloanthracen-13 (10*H*)-yl)acetamide **(1)** and (E)-ethyl 3-(4-chlorophenyl)-2-cyanoacrylate. The product was obtained after 16 hrs as white powder. Yield: 88 %, m. p.: 258-260 ºC. FTIR (KBr): ν/cm^{-1}= 3445 (OH), 3018 (CH-

aromatic), 2212 (CN),1775, 1715 (C=O) ; ^{1}H-NMR (DMSOd_6) δ (ppm) = 3.45-3.47 (d, d, 2H), 4.77-4.87 (d, d, 2H), 7.08-7.74, (m, 8H, Ar-H), 8.46 (s, 1H); ^{13}C NMR (100 MHz, DMSO-d_6): δ 44.47, 45.12, 45.60, 124.01, 125.76, 126.85, 127.16, 129.65, 130.39, 131.71, 137.59, 139.09, 142.34, 161.77, 173.23; MS (EI, 70 eV): m/z (%) = 547 (M+, 12 %); Chemical formula: $C_{31}H_{19}N_4O_4Cl$: (547.1); Calculated: C, 71.11; H, 3.33; N, 15.55, Cl, 6.48; Found: C, C, 71.12; H, 3.34; N, 15.57, Cl, 6.51.

2.2.5. 4-(3-nitrophenyl)-1-((11S,15R)-12,14-dioxo-11,12,14,15-tetrahydro-9H-9,10-[3,4]epipyrroloanthracen-13(10H)-yl)-6-hydroxy-2-oxo-1,2,3,4-tetrahydropyridine-3,5-dicarbonitrile (6).

It was prepared according to the general procedure using 2-cyano-*N*-((11*S*,15*R*)-12,14-dioxo-11,12,14,15-tetrahydro-9*H*-9,10-[3,4]epipyrroloanthracen-13 (10*H*)-yl)acetamide **(1)** and (E)-ethyl 3-(3-nitrophenyl)-2-cyanoacrylate. The product was obtained after 20 hrs as white powder. Yield: 81 %, m. p.: 250-252 ^{o}C .FTIR (KBr): ν/cm^{-1}= 3420 (OH), 3012 (CH-aromatic), 2220 (CN),1784, 1720 (C=O) ; ^{1}H-NMR (DMSOd_6) δ (ppm) = 3.40 (d, d, 2H), 4.89 (d, d, 2H), 7.15-8.53, (m, 8H, Ar-H), 8.85 (s, 1H); ^{13}C NMR (100 MHz, DMSO-d_6): δ 45.07, 45.33, 122.67, 124.79, 125.23, 126.86, 127.20, 131.16, 134.79, 139.57, 142.12, 148.70, 159.67, 173.08; MS (EI, 70 eV): m/z (%) = 557 (M+, 23 %); Chemical formula: $C_{31}H_{19}N_5O_6$: (557.6); Calculated: C, 71.11; H, 3.33; N, 15.55; Found: 71.12; H, 3.34; N, 15.57.

2.2.6. N-((11S,15R)-12,14-dioxo-11,12,14,15-tetrahydro-9H-9,10-[3,4] epipyrrolo -anthracen-13(10H)-yl)-2-imino-2H-chromene-3-carboxamide (7).

It was prepared according to the general procedure using 2-cyano-*N*-((11*S*,15*R*)-12,14-dioxo-11,12,14,15-tetrahydro-9*H*-9,10-[3,4]epipyrroloanthracen-13(10*H*)-yl)acetamide and salicylaldehyde . The product was obtained after for 12 hrs afforded white precipitate. Yield: 80 %, m. p.: 171-173 ^{o}C. FTIR (KBr): ν/cm^{-1}= 3348 (NH), 3009 (CH-aromatic),1781, 1717 (C=O); ^{1}H-NMR (DMSOd_6) δ (ppm) = 3.45-3.47 (d, d, 2H), 4.87 (d, d, 2H), 6.86-7.63, (m, 8H, Ar-H), 8.55 (s, 1H); ^{13}C NMR (100 MHz, DMSO-d_6): δ 44.58, 44.95, 45.10, 45.51, 117.02, 118.99, 120.65, 124.77, 125.19, 126.79, 127.10, 128.58, 134.46, 138.00, 139.85, 142.48, 158.13, 161.60, 169.06, 173.42 ; MS (EI, 70 eV): m/z (%) = 461 (M+, 31 %); Chemical formula: $C_{28}H_{19}N_3O_4$:(461.5); Calculated: C, 71.11; H, 3.33; N, 15.55; Found: C, 71.12; H, 3.34; N, 15.57.

2.3. Docking protocol.

The molecular docking approach was performed to modulate the antibacterial efficiency of the synthesized compounds toward DNA gyrase B chain [27]. The intermolecular bonds between the compounds and the active site residues of the target were studied using PyRx – virtual screening tool of Auto dock 4.2 [28]. The crystal structure of the target enzyme DNA gyrase B chain (PBD ID: 1KIJ) was downloaded from RCSB data bank. The obtained structure was optimized by removing water molecules and atomic clashes [29–35]. Further, the active site region was identified from the co-crystalline structure of the receptor-ligand complex. The grid was then generated around the active site pocket of the target enzyme for specific docking. In addition, the 2D chemical composition of the compounds was sketched using Chem Draw Ultra 7.0, then converted to SDF (Standard file format) using the Open Babel tool [36]. An in-house library of seven anthracene analogs was created for further

study. All the compounds were energy minimized using UFF (Universal Force Field) [37] to obtain structures with the proper bond length between different atoms and then used in the docking study. Enzyme-compound interactions of the complexes were examined in 2D and 3D styles, using Discovery studio 3.5 software. The physicochemical and chemical ADMET analyses of the compounds were calculated using Mol inspiration (https://molinspiration.com/) and admetSAR [38] (http://lmmd. ecust.edu.cn/ admetsar2), free web-based tools.

2.4. Determination of the minimum inhibitory concentration (MIC) and minimum bactericidal concentration (MBC) by INT reduction assay.

The determination of MIC and MBC were assayed as described earlier by Salem *et al*. [39]. The freshly prepared cultures of both *Escherichia coli* (Gram-negative bacteria) and *Bacillus cereus* (Gram-positive bacteria) were adjusted to OD_{595} of 0.001. 100 µL of each isolate culture was put into sterilized 96-well plates. Then 20 µL of the screened compounds (5 µg mL^{-1}) (serial dilutions of 10^{-1} -10^{-10} were used, and 8 replicates were made for each dilution into complete raw of the 96-well plate). The un-inoculated media was confirmed as a negative control after 24 h incubation at 37ºC. MIC was investigated by the addition of 40µL of p-iodonitrotetrazolium violet chloride (INT) (0.2 µg ml^{-1}, SIGMA-ALDRICH) to the plates and re-incubated at 37ºC for 30 min., the lowest concentration which banned color variation is the MIC [40]. The MBC was determined by transferring 50 mL from each well of overnight MIC plates (and/or higher) to sterile (TSA) fresh plates. Viable colonies were counted after 24 hrs at 37ºC. The limit of detection for this assay was 10^1 CFU/mL.

3. Results and Discussion

3.1. Chemistry.

Recently, our laboratory contributed to synthesizing new heterocyclic compounds such as arylidene, pyridine, chromene, and pyrazole derivatives [41, 42]. In which we proposed that anthracene derivatives **(1)** reacted with aromatic aldehydes, arylidenes, hydroxyl aldehydes, and hydrazine hydrate to afford the corresponding products [43].

In the present work, heating under reflux of 2-cyano-*N*-((11*S*,15*R*)-12,14-dioxo-11,12,14,15-tetrahydro-9*H*-9,10- [3,4]epipyrroloanthracen-13(10*H*)-yl) acetamide **(1)** with hydroxyl amine hydrochloride in ethanol in the existence of sodium acetate for 6 hrs produces (11*S*,15*R*)-13-((5-aminoisoxazol-3-yl)amino)-10,11-dihydro-9*H*-9,10-[3,4]epipyrrolo anthracene-12,14(13*H*,15*H*)-dione **(2)** in a 75 % yield, Scheme 1. The chemical composition of **(2)** was established according to the corresponding spectroscopic results. Therefore, the FTIR spectrum presented a typical peak at 3345 cm^{-1} for (NH) group and 1760, 1708 cm^{-1} for carbonyl groups. Also, the ^{1}H-NMR ($DMSOd_6$) δ (ppm) = 3.17- 3.20 (d, d, 2H), 4.62 (s, NH), 4.77 (d, d, 2H), 7.12 (s, 1H), 7.12-7.46 (m, 8H, Ar-H). Additionally, the mass spectrum (MS) exhibited the molecular ion peak (MIP) m/z=374 (M^+) attributed to the correct molecular formula $C_{21}H_{18}N_4O_3$. **T**he suggested mechanism for preparing compound **(2)** is represented in Scheme 2. Hydroxyl amine attacked the carbonyl group in compound **(1)** to afford intermediate **(I)**, then occurred intra cyclization reaction between the hydroxyl group and cyano group to form intermediate **(II)**, which under our conditions gave the compound **(2)** *via* oxidation process and elimination of water molecule.

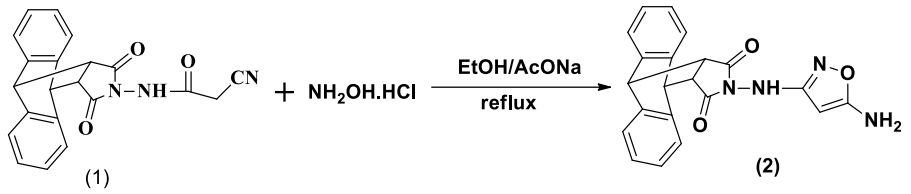

Scheme 1. Synthesis of compound **2**.

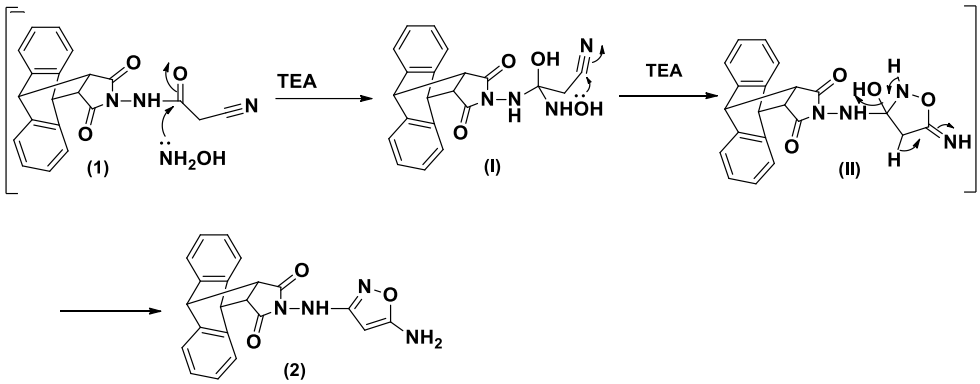

Scheme 2. Possible mechanism of compound **2** synthesis.

Interestingly, refluxing compound **(1)** with arylidene derivatives in ethanol as a solvent and TEA as a basic catalyst for the proper time afford new arylidene derivatives **(3,4)** in a 70-76% yield, respectively, Scheme 3. A plausible mechanism for this reaction is represented in Scheme 4. Active methylene under basic catalyst gave anion compound (**3I**), which reacted by β-attacked with arylidene derivatives under reaction condition afford iminocyclobutane carboxamide (**3II**) *via* witting like mechanism [44]. Finally, intermediate cyclobutane (**3II**) is converted to a compound (**3, 4**). On the other hand, the formation of compound (**3, 4**) is difficult due to the unshared electron pair of nitrogen atom it is unavailable, and in the presence of TEA gave anion compound which attacked the arylidene derivatives. Similarly, Aly and others have reported that the reaction of p-nitrobenzaldehyde as a carbonyl component with benzylidene malononitrile in acidified methanol afforded 2-(4-nitrobenzylidene) malononitrile *via* witting like mechanism [45].

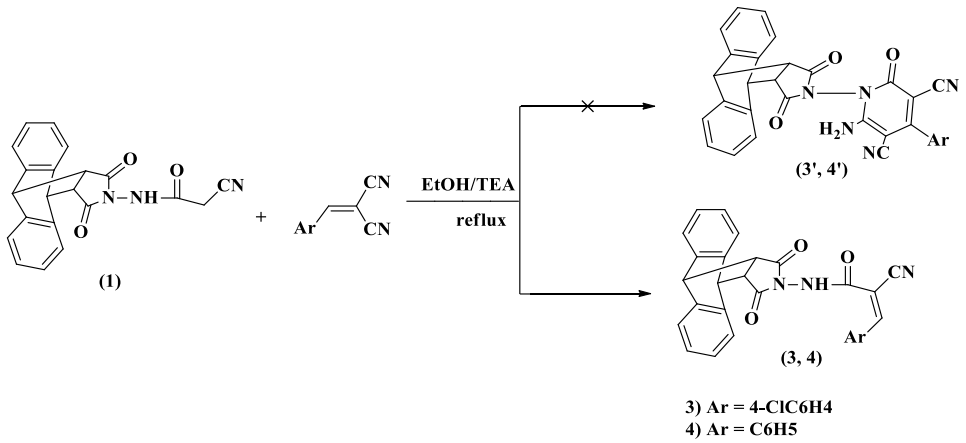

Scheme 3. Synthesis of arylidene derivatives **3, 4.**

Compounds **(3, 4)** were established according to their corresponding F-TIR analysis, ^{1}H-NMR, ^{13}C-NMR, and MS spectra. The FTIR spectra presented abs. frequencies at 3332-3345, 2205-2207, and 1785-1720 cm^{-1} that are equivalent to NH-, CN-, and -C=O groups, respectively. ^{13}C-NMR spectra of the compounds **(3, 4)** gave excellent suggestions for the chemical composition of these products. ^{13}C-NMR exhibited peaks due to CN-groups at the δ 124-125 ppm region, as well as the signals in the δ 169-173 ppm region due to -C=O groups.

^{1}H-NMR of compound (**3**) exhibited signals as δ (ppm) = 3.45 (d, d, 2H), 4.87 (d, d, 2H), 7.11-7.98 (m, 8H, Ar-H), 8.46 (s, 1H). Additionally, the MS showed the MIP at m/z=479 (M^{+}), corresponding to the molecular formula $C_{28}H_{18}N_3O_3Cl$. The ^{1}H-NMR spectrum of compound (**4**) showed δ (ppm) = 3.30-3.37 (d, d, 2H), 4.88 (d, d, 2H), 7.17-7.70 (m, 8H, Ar-H), 8.32 (s, 1H). The MS exhibited the MIP at m/z= 444 (M^{+}) corresponding to the molecular formula $C_{28}H_{18}N_3O_3$.

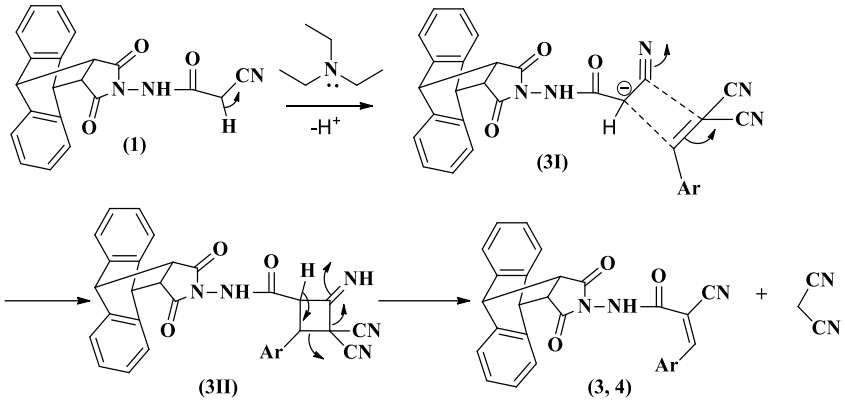

Scheme 4. Synthetic route of arylidene derivatives **3,4.**

Furthermore, the reaction of compound **(1)** with ethyl α-cyano-aryl-trans- cinnamate **(a, b**) (a, Ar = 4-ClC_6H_5 - b, Ar = 3-$NO_2C_6H_5$) in boiling ethanol in the presence of TEA furnished the corresponding product **(5)** and **(6)** in a 88% and 81% yield, respectively, Scheme 5. The suggested reaction mechanism is outlined in Scheme 6. The intramolecular reaction between –NH group and carbonyl group in carboxylate gave the cyclization product **(5,6)** *via* intermediate **(5I)** whereas the oxygen atom, not electron sank enough, in addition to the presence of (-OEt) as leaving group, in which converted to intermediate **(5II)**, then aromatization occurs to form the finally compound (Rout A). On the other hand, oxo-pentanoate intermediate **(5I)** converted to **(5III)** then by elimination of water afforded compound **(5VI)**, (Route B). The previous reaction under our conditions gave the compound **(5, 6),** and the analysis proves this result, whereas the ethyl group in compound **5VI** was not obtained in the ^{1}H-NMR analysis.

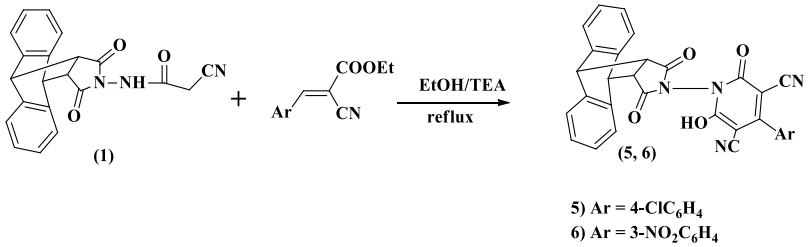

5) Ar = 4-ClC_6H_4
6) Ar = 3-$NO_2C_6H_4$

Scheme 5. Synthetic route for compounds **5 and 6.**

The CF of **5,** and **6** were established by their spectral analysis F-TIR, ^{1}H-NMR, ^{13}C-NMR, and MS. The FTIR spectra indicated absorption bands at 3445-3420, 2220-2212, and 1784-1715 cm^{-1} due to OH, CN and C=O groups, respectively. ^{13}C-NMR spectra of the compounds **(5, 6)** provided a great suggestion for these compounds' chemical Formula (CF) corresponding to their stereochemistry. ^{13}C-NMR exposed signals due to C≡N groups at the region of δ 122-124 ppm, and signals in the δ 159-173 ppm region due to -C=O groups. The ^{1}H-NMR spectrum of compound (**5**) indicated δ (ppm) = 3.45-3.47 (d, d, 2H), 4.77-4.87 (d, d, 2H), 7.08-7.74, (m, 8H, Ar-H), 8.46 (s, 1H). Furthermore, the MS exhibited the MIP at m/z= 547 (M^{+}), corresponding to the molecular formula $C_{31}H_{19}N_4O_4$. The ^{1}H-NMR spectrum of

compound **(6)** showed δ (ppm) = 3.40 (d, d, 2H), 4.89 (d, d, 2H), 7.15-8.53, (m, 8H, Ar-H), 8.85 (s, 1H). The MS showed the MIP at m/z= 557(M^+) represented by the molecular formula $C_{31}H_{19}N_5O_6$.

It is worth mentioning that refluxing a one-pot three components reaction of compound **(1)**, benzaldehyde, and malononitrile with heating in ethanol in the existence of TEA as a catalyst for 18 hrs afforded the compound **(4)** in an 80% yield, Scheme 7.

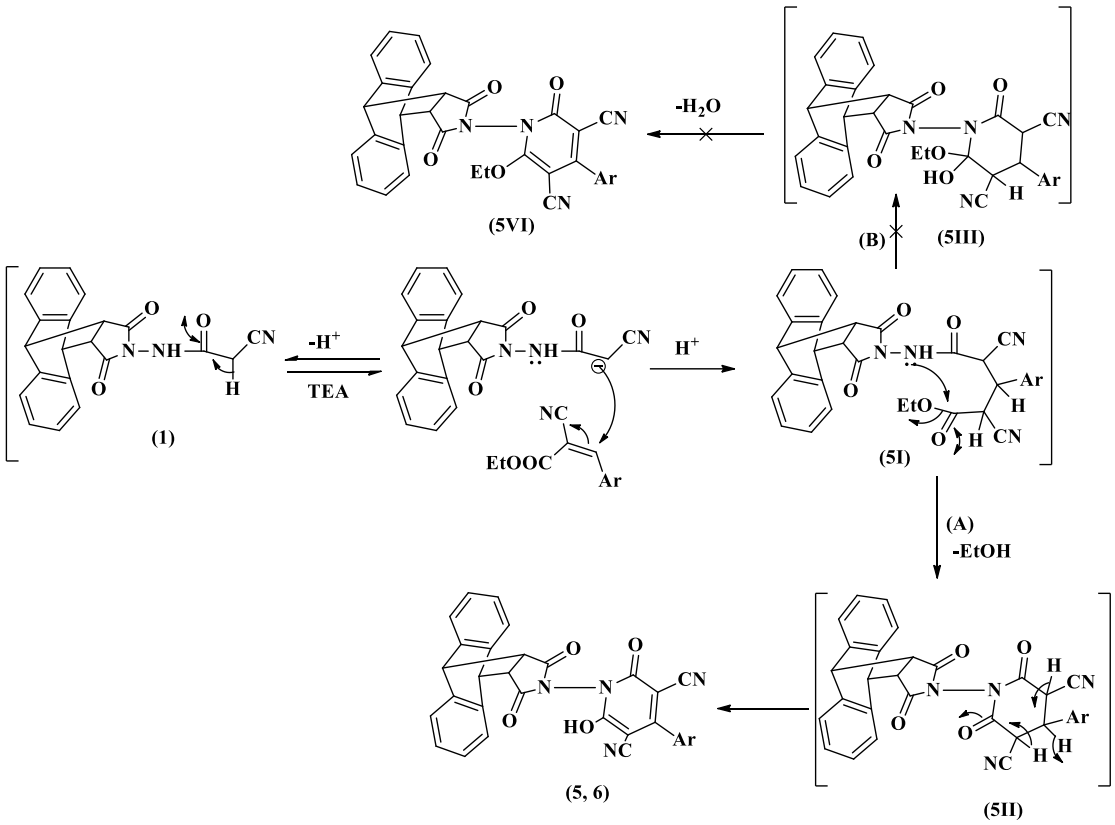

Scheme 6. The synthetic strategy of analogs **5** and **6.**

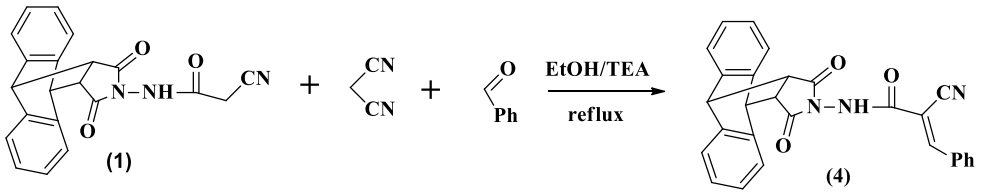

Scheme 7. Synthesis of compound 4 through one pot three components reaction.

In the previous work, our group [46] reported that the reaction of 2-hydroxyl-1-naphtaldehyde with the compound **(1)** as a precursor active methylene afforded a cyclization product. Here, we preferred to use salicylaldehyde instead of 2-hydroxyl-1-naphtaldehyde to decrease the bulky group. Refluxing an equimolar ratio, the mixture of compound **(1)** and salicylaldehyde in ethanol in the existence of triethanol amine (TEA) for 12 hrs provided the compound **(7)** as a soul product in an 80% yield, Scheme 8. The possible reaction mechanism is represented in Scheme 9.

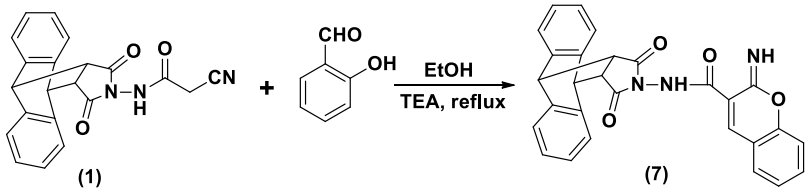

Scheme 8. Synthesis of compound **7**.

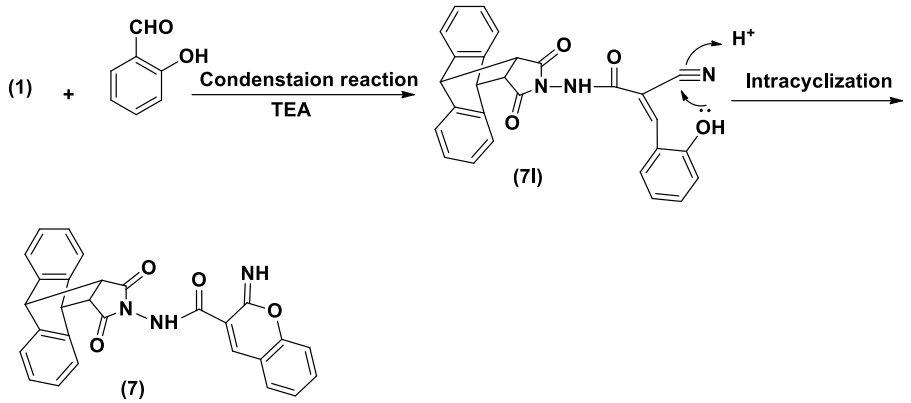

Scheme 9. The suggested mechanism of formation of compound **7**.

The chemical structure of **(7)** was confirmed depending on its spectroscopic data. Compound **6** showed abs. frequencies at 3348 cm^{-1} that related to NH-group and characteristic absorption bands for (C=O) groups at 1781and 1717 cm^{-1}. The ^{1}H-NMR spectrum of compound **(7)** δ (ppm) = 3.45-3.47 (d, d, 2H), 4.87 (d, d, 2H), 6.86-7.63, (m, 8H, Ar-H), 8.55 (s, 1H). ^{13}C-NMR spectrum for compound **(7)** fit the proposed structure well, as the diverse carbon atoms resulting from the benzene rings, and carbonyl groups were examined. Moreover, the MS showed the MIP m/z=461 (M^{+}) attributed to the $C_{28}H_{19}N_3O_4$ formula.

3.2. Docking study and SAR analysis.

The DNA gyrase enzyme plays an important role in the viability of bacterial cells [47]. It has ATPase activity, giving a sufficient amount of energy for DNA supercoiling [48]. Bacterial DNA gyrase is the target of many antibiotics, such as ciprofloxacin and Novobiocin [49]. Therefore, in the present study, DNA gyrase B chain has been selected as a promising target for identifying new, potential, and less toxic antimicrobial agents. The molecular docking estimations of the compounds **1-7** and the active site of the target DNA gyrase B chain enzyme were achieved. In addition, Novobiocin was selected as a standard drug to compare the docking score with theses of these synthesized compounds. Herein, PyRx- virtual screening software 0.8 [28] was used to simulate the compound into the active site of the enzyme in order to calculate the free binding energy (ΔG) of the interaction between each other. The docking scores were expressed in negative energy terms (kcal/mol) and ranked depending on the higher negative value indicating better closeness toward the target [30,47, 50].

Computer-based docking technique exhibited nine poses for each complex [51, 52], and the preferable binding orientation between enzyme and compound, with a more negative score, was considered for further study. Data presented in Table 1 displayed the binding energy, types of intermolecular interaction, in addition to bond lengths. The docking results revealed compound 1, bound to the target enzyme through one hydrogen bond and one arene-σ interaction with Asn45 and Ile77 at 2.89 and 3.95 Å, respectively. Compound **2**, was nicely docked to the target binding site *via* incorporation of two hydrogen bonds and one arene -cation interaction with Gly116, Thr336, and Lys109 at the distances of 2.25, 2.49, and 4.86 Å, respectively. Introducing electron-withdrawing groups (-Cl) on the phenyl ring causes less activity of the compounds [53, 54]. In this regard, compound **4** with phenyl ring showed binding energy of -9.4 kcal/mol, and formed an H-bond interaction with Lys102 at 2.98 Å. On the other hand, the analog **3** with an electron-withdrawing group (-11.3 kcal) exhibited two hydrogen bond interactions with the residue Asn45 at 3.18 and 2.88 Å, respectively. The compound **5** with chlorine atom at para position (-10.7 kcal/mol) showed arene-stacked

interactions such as T-shaped arene-arene and arene-cation with the amino acid residues Phe103, Lys102, and Lys109 at 4.47 (edge to face), 4.87 and 5.98 Å, respectively. In addition, compound **6** with an electron-withdrawing group (–NO_2) at meta position (-10.0 kcal/mol) exhibited H-bond, T-shaped arene-arene, and arene-cation interactions to the amino acid residues Lys102, Phe103, and Lys109, respectively, at the distances of 2.97, 4.41 and 5.95 Å, respectively. Finally, compound **7,** with the binding energy of -10.9 kcal/mol, docked with Lys109 through two H-bonds and one arene-cation interaction at 3.09, 2.89, and 3.75 Å, respectively.

On the other hand, Novobiocin exhibited binding energy of -10.8 kcal/mol, which is closer to the synthesized compounds, and formed various types of interactions like H-bonds and arene-stacked with the amino acid residues Ala107, Lys109, Thr336, and Pro328 at distances 2.95, 2.98, 2.94, 2.93, 2.98, 3.94, 3.95, and 4.51 Å, respectively.

Lipinski's rule of five (RO5) [55] is used to determine the properties that would make a chemical compound like an orally active drug in human beings. The physicochemical and ADMET properties of the screened compounds are computationally predicted and listed in Tables 2 and 3. It can be observed that all synthetic compounds obey Lipinski's rule of five. Further, *in silico* artificial membrane permeation across Caco-2 cells was predicted for all synthesized compounds. It has been found that the passive transmembrane permeation of compounds exhibited good permeability values (78.81-83.94 nm/s). In addition, toxicity and carcinogenicity tests data declared that all compounds are non-toxic and non-carcinogenic. Therefore, the overall *in silico* ADME prediction appears favorable for future lead optimization.

3.3. The biological applications.

To confirm the docking study and SAR analysis as a potential source for antimicrobial activities, all the tested compounds 1-7 were tested for their antibacterial activity against the Gram-negative bacteria (*Escherichia coli*) and Gram-positive bacteria (*Bacillus cereus*). Both MIC and MBC values showed promising results for all the tested compounds, as represented in Table 4. The MIC values of the two tested bacteria ranged from 1 to 2 µg/mL. At the same time, the recorded MBC values ranged from 2 to 3 µg/mL.

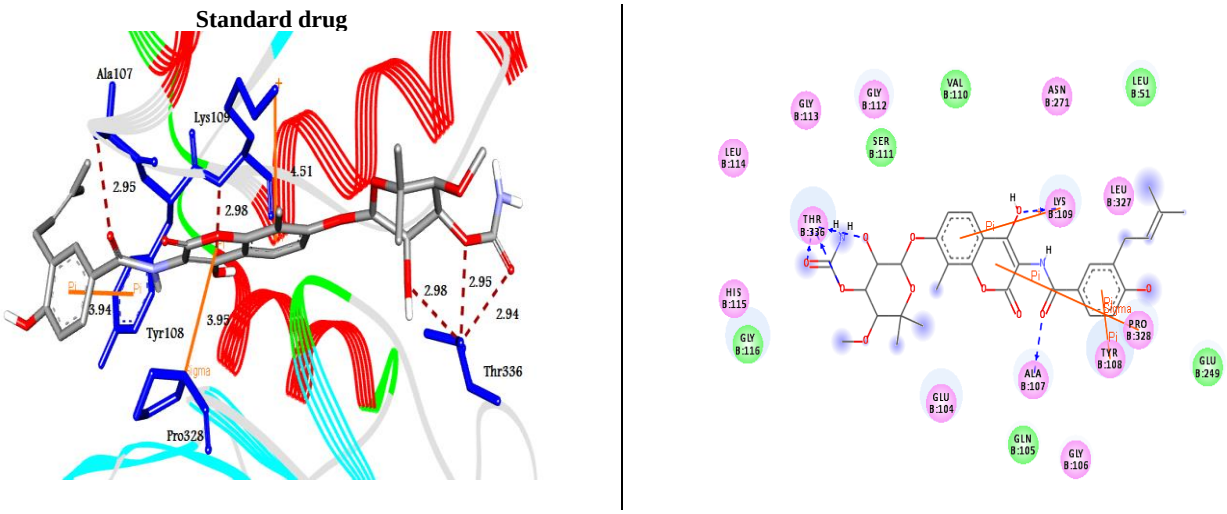

Compound 1

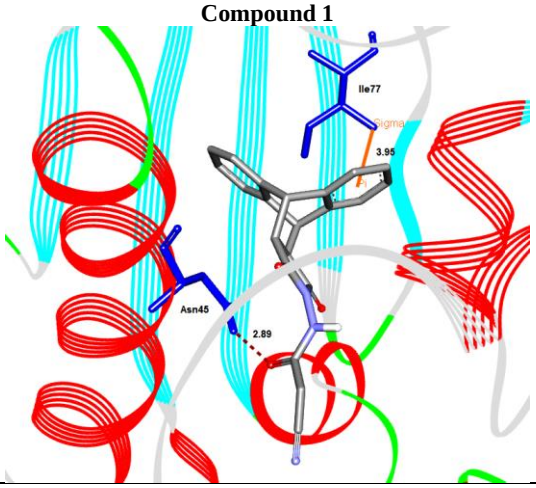

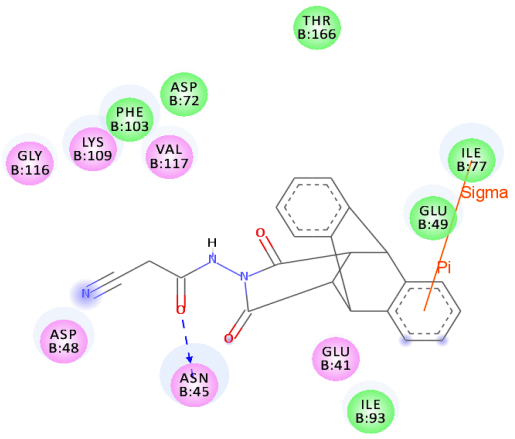

Compound 2

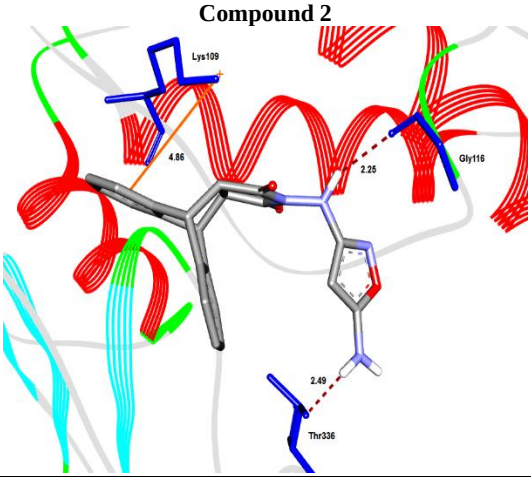

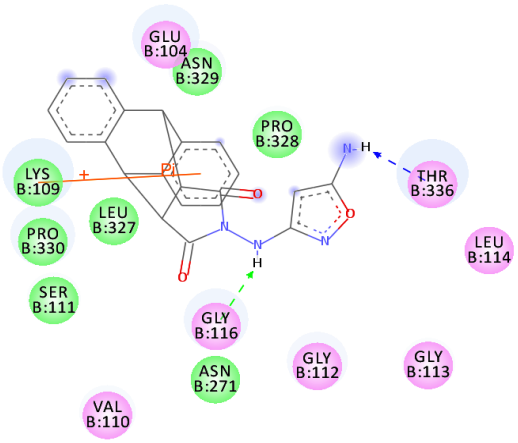

Compound 3

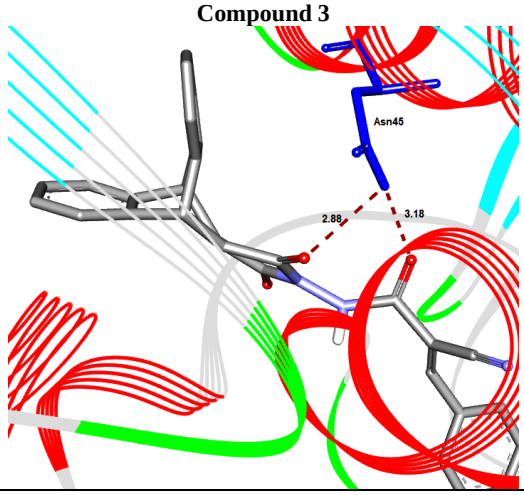

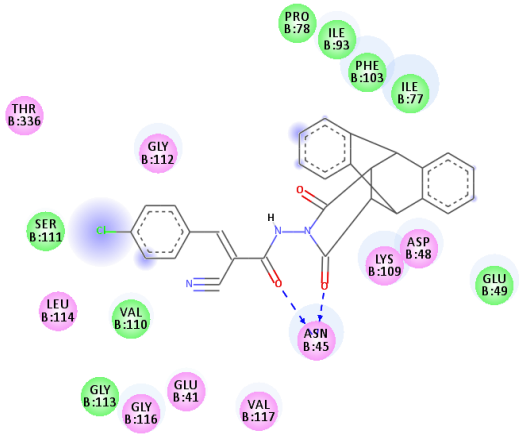

Compound 4

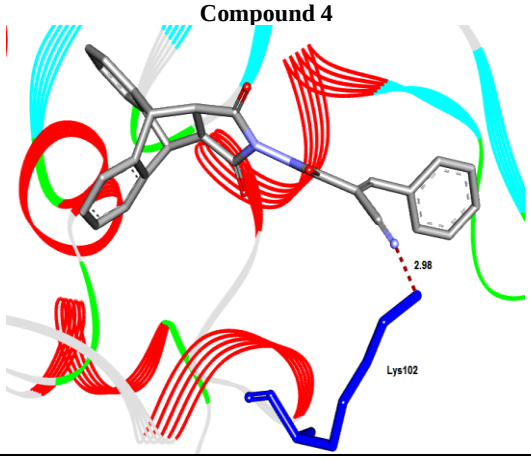

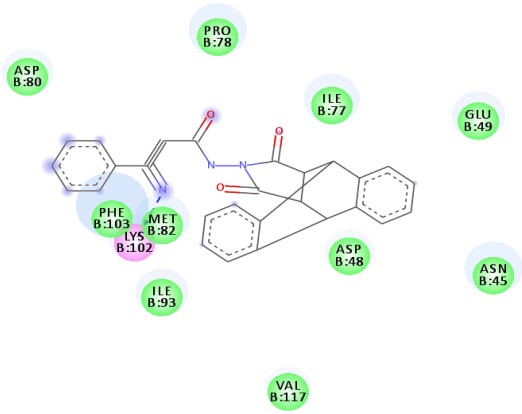

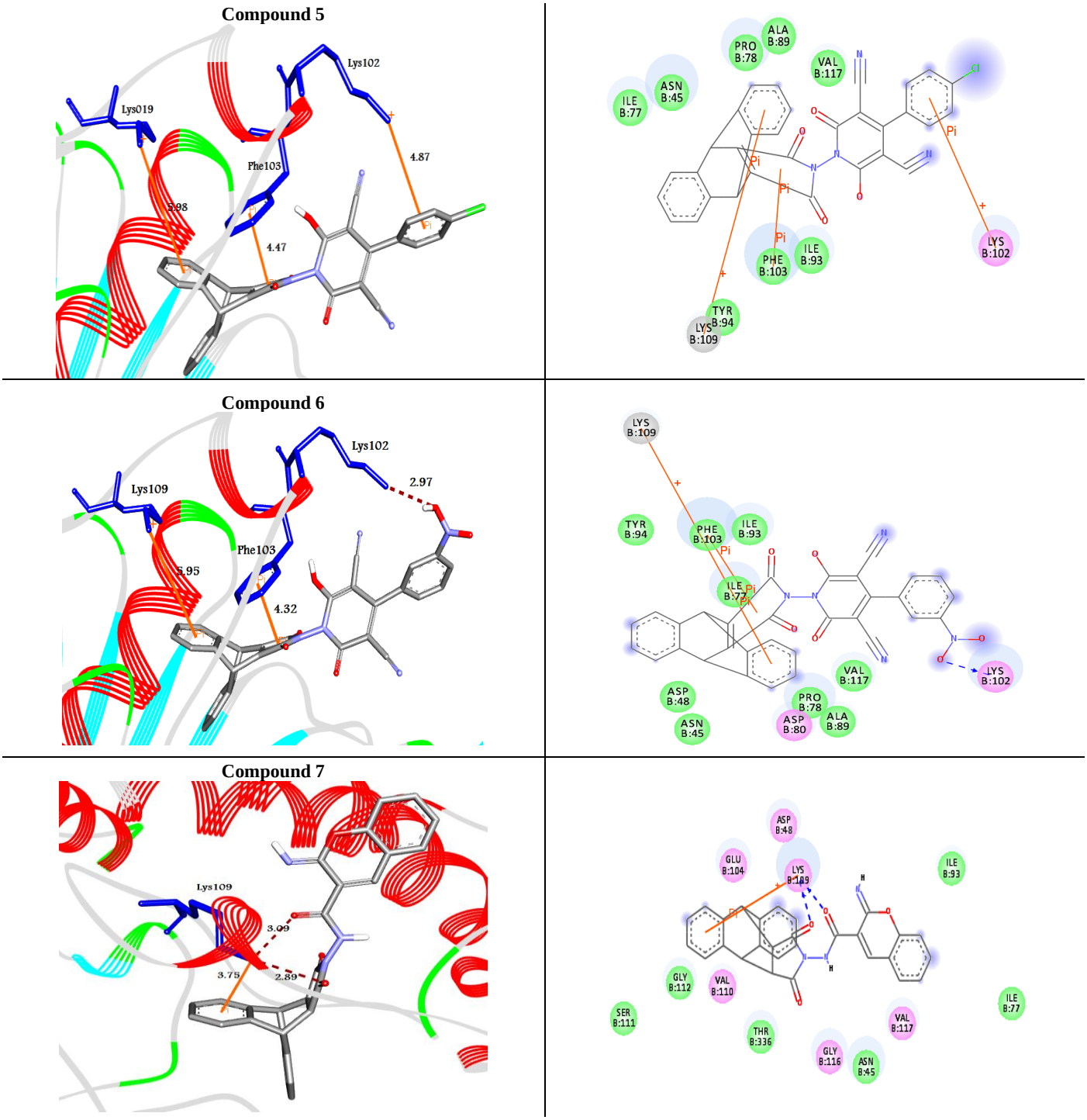

Figure 1. (**A**) 3D, (**B**) 2D representations of all docked complexes. (**A**) H-bonds are represented in red dotted lines, while pi-interactions are shown in orange lines. (**B**) H-bonds are represented in blue dotted lines, while pi-interactions are shown in orange lines.

Interestingly, both Gram-negative and Gram-positive bacteria were sensitive to the compounds. The antimicrobial activity can be modulated by the presence of anthracene moiety, electron-withdrawing groups, and amide linkage.

Table 1. The binding energies of the standard drug and synthesized compounds **1-7** and their molecular interactions with the active site of the target protein.

	Structure	Binding Energy kcal/mol	Docked complex (amino acid–ligand) interactions	Distance (Å)
Ref. drug	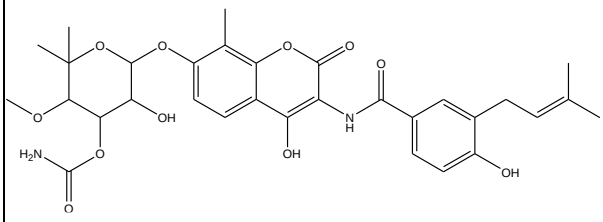	-10.8	**H-bond** ALA107:N---Ref drug LYS109:N---Ref drug THR336:OG1---Ref drug THR336:OG1---Ref drug THR336:OG1---Ref drug **arene- arene** TYR108---Ref drug **arene-σ** PRO328:CA---Ref drug **arene- cation** LYS109:NZ---Ref drug	 2.95 2.98 2.94 2.95 2.98 3.94 3.95 4.51
1	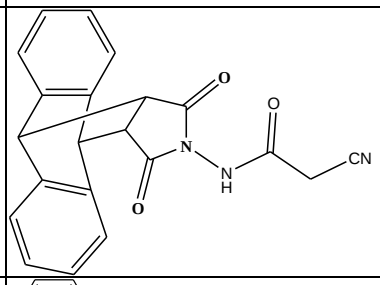	-8.4	**H-bond** ASN45:ND2---compound**1** **arene-σ** ILE77:CG2---compound**1**	 2.89 3.95
2	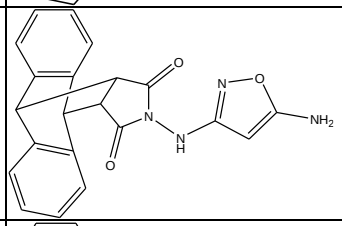	-9.9	**H-bond** GLY116:O---compound **2** THR336:OG1---compound **2** **arene- cation** LYS109:NZ---compound **2**	 2.25 2.49 4.86
3	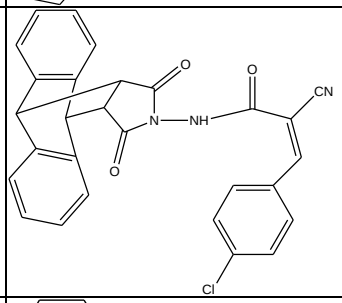	-11.3	**H-bond** ASN45:ND2---compound **3** ASN45:ND2---compound **3**	 2.88 3.18
4	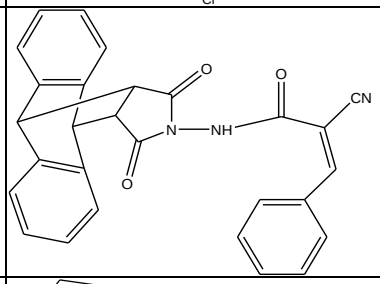	-9.4	**H-bond** LYS102:NZ---compound **4**	 2.98
5	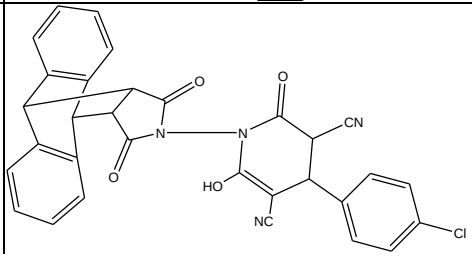	-10.7	**arene- arene** PHE103---compound **5** **arene- cation** LYS102:NZ---compound **5** LYS109:NZ---compound **5**	 4.47 4.87 5.98

	Structure	Binding Energy kcal/mol	Docked complex (amino acid–ligand) interactions	Distance (Å)
6	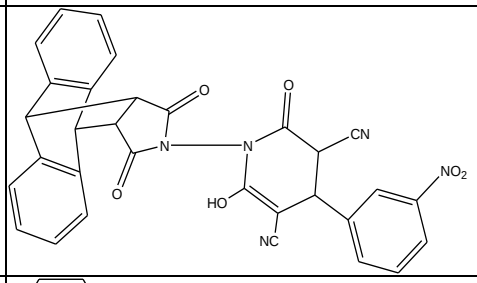	-10.0	**H-bond** LYS102:NZ---compound **6** **arene- arene** PHE103---compound **6** **arene- cation** LYS109:NZ---compound **6**	 2.97 4.41 5.95
7	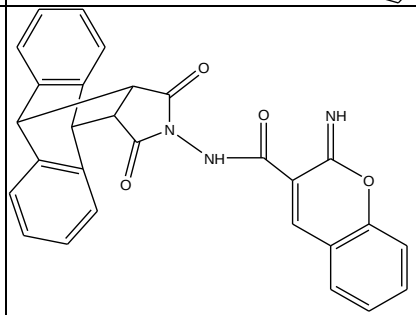	-10.9	**H-bond** LYS109:NZ---compound **7** LYS109:NZ---compound **7** **arene- cation** LYS109:NZ---compound **7**	 3.09 2.89 3.75

Table 2. Physicochemical properties of the title compounds **1-7.**

Compd. No.	milogp ≤5	TPSA ≤140	MW 130-725	n_{ON} 2.0-20.0	n_{OHNH} 0.0-6.0	$n_{rotb.}$ ≤10	Vol A^3
1	0.88	90.27	357.37	6	1	2	360.04
2	2.01	101.46	372.38	7	3	2	313.50
3	4.17	90.27	479.92	6	1	3	401.60
4	3.50	90.27	445.48	6	1	3	388.06
5	3.76	125.50	546.97	8	1	2	446.76
6	3.01	171.32	557.52	11	1	3	459.47
7	1.03	103.47	461.48	7	2	2	391.64

milogp, logarithm ratio of partition coefficient between n-octanol and water; TPSA, topological polar surface area; MW, molecular weight; n_{ON}, number of hydrogen bond acceptors; n_{OHNH}, number of hydrogen bond donors; $n_{rotb.}$, number of rotatable bonds.

Table 3. List of ADMET properties of molecules **1-7.**

	Blood-Brain Barrier (BBB^+)	Caco-2 Permeability ($Caco^{2+}$)	%Human Intestinal Absorption (HIA^+)	AMES toxicity	Carcinogenicity
Reference range	**-3 to 1.2**	**<25 is poor >500 is great**	**<25 is poor >80% is high**	**Nontoxic**	**Non carcinogenic**
1	0.98	82.50	98.90	Non-toxic	Non carcinogenic
2	0.97	82.77	96.55	Non-toxic	Non carcinogenic
3	0.98	83.26	92.90	Non-toxic	Non carcinogenic
4	0.97	83.94	92.88	Non-toxic	Non carcinogenic
5	0.98	83.66	97.30	Non-toxic	Non carcinogenic
6	0.97	82.50	97.60	Non-toxic	Non carcinogenic
7	0.97	78.81	94.06	Non-toxic	Non carcinogenic

The pharmacokinetic parameters of compounds are evaluated using admetSAR.

Table 4. Antimicrobial screening results of molecules **1-7.**

Bacteria/ Compound	*Escherichia coli*		*Bacillus cereus*	
	MIC/ MBC*			
1	**1.0**±0.0 /	**1.5** ± 0.0	**1.0**± 0.0 /	**2.0** ± 0.0
2	**1.0**± 0.0 /	**1.5** ± 0.2	**1.0**± 0. 1 /	**1.5** ± 0.2
3	**2.0**± 0.0 /	**2.0** ± 0.1	**2.0**± 0.2 /	**2.0** ± 0.2
4	**2.0**± 0.1 /	**2.5** ± 0.1	**2.0**± 0.1 /	**2.5** ± 0.1
5	**1.0**± 0.0 /	**2.0** ± 0.0	**1.0**± 0.0 /	**2.0** ± 0.0
6	**1.0**± 0.1 /	**1.5** ± 0.1	**1.0**± 0.1 /	**2.0** ± 0.1
7	**2.0**± 0.1 /	**2.0** ± 0.2	**2.0**± 0.0 /	**2.0** ± 0.2

*MIC: Minimum inhibitory concentration (μg mL^{-1}); MBC: Minimum bactericidal concentration (μg mL^{-1}).

4. Conclusions

In summary, a sequence of arylidene, pyridine, oxazole, and chromene derivatives containing anthracene moiety has been prepared and characterized by FT-IR, ^{1}H-NMR, ^{13}C-NMR, and MS. Several computational tools such as molecular docking, SAR, and ADMET analysis are used to identify DNA gyrase inhibitors. In addition, all compounds were evaluated for their antibacterial activity against various strains. Looking at the biological activity, all compounds exhibited promising activity against Gram-negative bacteria (*Escherichia coli*) and Gram-positive bacteria (*Bacillus cereus*). Overall, the *in silico* and experimental findings suggest that anthracene hybrid molecules **1-7** can be used as potential drug candidates to treat infectious diseases.

Funding

This research received no external funding.

Acknowledgments

The authors are gratefully acknowledged Prof. Wesam Salem and Dr. Doaa Azab, Botany and Microbiology Department, Faculty of Science, South Valley University, for their help in biological work.

Conflicts of Interest

The authors declare that they have no conflict of interest or competing interests.

References

1. Schiel, M.A.; Silbestri, G.F.; Alvarez, M.B.; Domini, C.E. Ultrasound-promoted metal-catalyzed synthesis of heterocyclic compounds of medicinal interest. *In: Green Synthetic Approaches for Biologically Relevant Heterocycles* **2021**, *1*, 461-496, https://doi.org/10.1016/B978-0-12-820586-0.00002-9.
2. Gujjarappa, R. *et al*. An Overview on Biological Activities of Oxazole, Isoxazoles and 1,2,4-Oxadiazoles Derivatives. *In: Swain, B.P. (eds) Nanostructured Biomaterials. Materials Horizons: From Nature to Nanomaterials* **2022**, Springer, Singapore, https://doi.org/10.1007/978-981-16-8399-2_10.
3. Albratty, M.; Alhazmi, H.A. Novel pyridine and pyrimidine derivatives as promising anticancer agents: A review. *Arab. J. Chem.* **2022**, *15*, 103846, https://doi.org/10.1016/j.arabjc.2022.103846.
4. Abu-Hashem, A.A.; Fathy, U.; Gouda, M.A. Synthesis of 1,2,4-triazolopyridazines, isoxazolofuropyridazines, and tetrazolopyridazines as antimicrobial agents. *J. Heterocycl. Chem.* **2020**, *57*, 3461–3474, https://doi.org/10.1002/jhet.4065.
5. Mishra, S.; Patel, S.; Halpani, C.G. Recent Updates in Curcumin Pyrazole and Isoxazole Derivatives: Synthesis and Biological Application. *Chem. Biodivers.* **2019**, *16*, e1800366, https://doi.org/10.1002/cbdv.201800366.
6. Orlando,T.; Salbego, P.R.S.; Farias, F.F.S.; Weimer, G.H.; Copetti, J.P.P.; Bonacorso, H.G.; Zanatta, N.; Hoerner, M.; Berná, J.; Martins, M.A.P. Crystallization Mechanisms Applied to Understand the Crystal Formation of Rotaxanes. *European J. Org. Chem.* **2019,** *21*, 3451–3463, https://doi.org/10.1002/ejoc.201801870.
7 Rashdan, H.R.M.; Abdel-Aziem, A.; El-Naggar, D.H.; Nabil, S. Synthesis and biological evaluation of some new pyridines, isoxazoles and isoxazolopyridazines bearing 1,2,3-triazole moiety. *Acta Pol. Pharm.-Drug Res.* **2019**, *76*, 469–482, http://dx.doi.org/10.32383/appdr/103101.
8. Kasthuri, M.; Li, C.; Verma, K.; Russell, O.O.; Dickson, L.; McCormick, L.; Bassit, L.; Amblard, F.; Schinazi, R.F. Synthesis of 4'-substituted-2'-deoxy-2'-α-fluoro nucleoside analogs as potential antiviral agents. *Molecules* **2020**, *25*, 1258, https://doi.org/10.3390/molecules25061258.

9. Asif, M.; Imran, M.; Abida. Antimicrobial Activities of Various Thiazine Based Heterocyclic Compounds: A Mini-Review. *Mini Rev Org Chem.* **2022**, *19*, 166-172, http://dx.doi.org/10.2174/1570193X18666210629102447.
10. Nayak, Y.N.; Gaonkar, S.L.; Saleh, E.A.M. *et al.* Chloramine-T (N-chloro-p-toluenesulfonamide sodium salt), a versatile reagent in organic synthesis and analytical chemistry: An up to date review. *J. Saudi Chem. Soc.* **2022**, *26*, 101416, https://doi.org/10.1016/j.jscs.2021.101416.
11. Trivedi, H.D.; Joshi, V.B.; Patel, B.Y. Pyrazole Bearing Pyrimidine Analogues as the Privileged Scaffolds in Antimicrobial Drug Discovery: A Review. *Anal. Chem. Lett.* **2022**, *12*, 147-173, https://doi.org/10.1080/22297928.2021.1910565.
12. Turones, L.C.; Martins, A.N.; Moreira, L.K. da S.; Fajemiroye, J.O.; Costa, E.A. Development of pyrazole derivatives in the management of inflammation. *Fundam. Clin. Pharmacol* **2021**, *35*, 217-234, https://doi.org/10.1111/fcp.12629.
13. Moustafa, A.H.; El-Sayed, H.A.; El Rayes, S.M.; Morsy, H.A.; Abd-allah, S.H.; Ismail, H.F.; Abd El-Aal, M.M. Pyrazoles and Isoxazoles Based Sulfanilamide and Phenazone as Antimicrobial Agents: Synthesis and Biological Activity. *Russ. J. Gen. Chem* **2019**, *89*, 2314–2320, https://doi.org/10.1134/S1070363219110240.
14. Wu, Y.D.; Guo, Z.G.; Deng, W.J.; Wang, J.G. SD0006 promotes nucleus pulposus cell proliferation via the p38MAPK/HDAC4 pathway. *Eur. Rev. Med. Pharmacol. Sci.* **2020**, *24*, 10966–10974, https://doi.org/10.26355/eurrev_202011_23580.
15. Dasari, S.R.; Tondepu, S.; Vadali, L.R.; Seelam, N. PEG-400 mediated an efficient eco-friendly synthesis of new isoxazolyl pyrido[2,3-d]pyrimidines and their anti-inflammatory and analgesic activity. *Synth. Commun.* **2020**, *50*, 2950-2961, https://doi.org/10.1080/00397911.2020.1787449.
16. Yakantham, T.; Sreenivasulu, R.; Alluraiah, G.; Tej, M.B.; Ramesh Raju, R.; Design, Synthesis, and Anticancer Activity of 1,2,3-Triazole Likned Thiazole-1,2-isoxazole Derivatives. *Russ. J. Gen. Chem.* **2019**, *89*, 2522–2527, https://doi.org/10.1134/S1070363219120314.
17. Saadati-Moshtaghin, H.R.; Maleki, B.; Tayebee, R.; Kahrobaei, S.; Abbasinohoji, F. 6-methylguanamine-Supported $CoFe_2O_4$: An Efficient Catalyst for One-Pot Three-Component Synthesis of Isoxazol-5(4H)-One Derivatives. *Polycycl. Aromat. Compd.* **2020**, *42*, 885-896, https://doi.org/10.1080/10406638.2020.1754865.
18. Donaire-Arias, A.; Montagut, A.M.; Puig de la Bellacasa, R.; Estrada-Tejedor, R.; Teixidó, J.; Borrell, J.I. 1H-Pyrazolo [3,4-b] pyridines: Synthesis and Biomedical Applications. *Molecules* **2022**, *27*, 2237, https://doi.org/10.3390/molecules27072237.
19. Singh, G.; Diksha; Mohit *et al*. Pyridine derived organosilatranes and their silica nanoparticles as "Turn-on" fluorescence sensor for selective detection of Zn^{2+} ions and their cytotoxicity evaluation. *Inorg. Chim. Acta* **2022**, *537*, 120926, https://doi.org/10.1016/j.ica.2022.120926.
20. Acharya, P.T.; Jethava, D.J.; Vasava, M.S.; Bhavsar, Z.A.; Bhoi, M.N.; Rajani, D.P.; Patel, H.D. Synthesis, docking study and biological evaluation of novel N- (1,3-benzothiazole). *Indian Journal of Chemistry - Section B (IJC-B)* **2020**, *59*, 1721–1737, http://nopr.niscair.res.in/handle/123456789/55644.
21. Jindal, S., Meena, K.; Magoo, D. Acetic acid catalysed solvent-free synthesis of spiro-isoxazolo[5,4-b]pyridines/quinolines by mechano-chemical grinding. *J. Heterocycl. Chem.* **2020**, *57*, 4271–4277, https://doi.org/10.1002/jhet.4133.
22. Su, C.; Liu, C.; Wang, Y.; Xiang, W.S.; Zou, C.G.; Huang, S.X. A new heliquinomycin analogue with immunosuppressive activity from Streptomyces sp. Jys28. *Rec. Nat. Prod.* **2019**, *13*, 456–461, http://dx.doi.org/10.25135/rnp.123.18.12.1085.
23. Keshavarz, R.; Farahi, M.; Karami, B. Efficient and Facile Synthesis of Chromenopyrano [2, 3-b] pyridine Derivatives Catalyzed by Sodium Carbonate. *Acta Chim. Slov.* **2021**, *68*, 332-340.
24. Youseftabar-Miri, L.; Hosseinjani-Pirdehi, H.; Akrami, A.; Hallajian, S. Recent investigations in the synthesis of spirooxindole derivatives by Iranian researchers. *J. Iran. Chem. Soc.* **2020**, *17*, 2179–2231, http://dx.doi.org/10.1007/s13738-020-01921-2.
25. Abdel Hamid, M.A.; El-Sayed, H.A.; Mohammed, S.M.; Moustafa, A.H.; Morsy, H.A. Functionalization of 1,2,3-Triazole to Pyrimidine, Pyridine, Pyrazole, and Isoxazole Fluorophores with Antimicrobial Activity. *Russ. J. Gen. Chem.* **2020**, *90*, 476–482, http://dx.doi.org/10.1134/S1070363220030226.
26. Reece, R.J.; Maxwell, A. DNA gyrase: Structure and function. *Crit. Rev. Biochem. Mol. Biol.* **1991**, *26*, 335–375, https://doi.org/10.3109/10409239109114072.
27. El-Saghier, A.M.; El-Naggar, M.; Hussein, A.H.M.; El-Adasy, A.B.A.; Olish, M.; Abdelmonsef, A.H. Eco-Friendly Synthesis, Biological Evaluation, and *In silico* Molecular Docking Approach of Some New

Quinoline Derivatives as Potential Antioxidant and Antibacterial Agents. *Front. Chem.* **2021**, *9*, 679967, https://doi.org/10.3389/fchem.2021.679967.
28. Dallakyan, S.; Olson, A.J. Small-Molecule Library Screening by Docking with PyRx. *Chem. Biol.* **2015**, *1263*, 243–250, https://doi.org/10.1007/978-1-4939-2269-7_19.
29. Abdelmonsef, A.H. Computer-aided identification of lung cancer inhibitors through homology modeling and virtual screening. *Egypt. J. Med. Hum. Genet.* **2019**, *20*, 6, https://doi.org/10.1186/s43042-019-0008-3.
30. Rondla, R.; Padmarao, L.S.; Ramatenki, V.; Haredi-Abdel-Monsef, A.; Potlapally, S.R.; Vuruputuri, U. Selective ATP competitive leads of CDK4: Discovery by 3D-QSAR pharmacophore mapping and molecular docking approach. *Comput. Biol. Chem.* **2017**, *71*, 224–229, https://doi.org/10.1016/j.compbiolchem.2017.11.005.
31. Abdelmonsef, A.H.; Mosallam, A.M. Synthesis, *in vitro* biological evaluation and *in silico* docking studies of new quinazolin-2,4-dione analogues as possible anticarcinoma agents. *J. Heterocycl. Chem.* **2020**, *57*, 1637-1654, https://doi.org/10.1002/jhet.3889.
32. Dasari, T.; Kondagari, B.; Dulapalli, R.; Abdelmonsef, A.H.; Mukkera, T.; Padmarao, L.S.; Malkhed, V.; Vuruputuri, U. Design of novel lead molecules against RhoG protein as cancer target–a computational study. *J. Biomol. Struct. Dyn.* **2017**, *35*, 3119–3139, https://doi.org/10.1080/07391102.2016.1244492.
33. Shehadi, I.A.; Rashdan, H.R.M.; Abdelmonsef, A.H. Homology modeling and virtual screening studies of antigen MLAA-42Protein: Identification of noveldrugcandidates against leukemia-an *in silico* approach. *Comput. Math. Methods Med.* **2020**, *2020*, 8196147, https://doi.org/10.1155/2020/8196147.
34. Wojtkowiak, K.; Jezierska, A.; Panek, J.J. Interactions between Artificial Channel Protein,Water Molecules and Ions Based on Theoretical Approaches. *Symmetry* **2022**, *14*, 691, https://doi.org/10.3390/sym14040691.
35. Sato, M.; Nakamura, S.; Inada, E.; Takabayashi, S. Recent Advances in the Production of Genome-Edited Rats. *Int. J. Mol. Sci.* **2022**, *23*, 2548, https://doi.org/10.3390/ijms23052548.
36. O'Boyle, N.M. *et al.* Open Babel: An Open chemical toolbox. *J. Cheminform.* **2011**, *3*, 33, https://doi.org/10.1186/1758-2946-3-33.
37. Rappé, A.K.; Casewit, C.J.; Colwell, K.S.; Goddard, W.A.; Skiff, W.M. UFF, a Full Periodic Table Force Field for Molecular Mechanics and Molecular Dynamics Simulations. *J. Am. Chem. Soc.* **1992**, *114*, 10024–10035, https://doi.org/10.1021/ja00051a040.
38. Cheng, F.; Li, W.; Zhou, Y.; Shen, J.; Wu, Z.; Liu, G.; Lee, P.W.; Tang, Y. AdmetSAR: A comprehensive source and free tool for assessment of chemical ADMET properties. *J. Chem. Inf. Model.* **2012**, *52*, 3099–3105, https://doi.org/10.1021/ci300367a.
39. Salem, W.M.; Shibat El-hamed, D.M.W.; Sayed, W.F.; Elamary, R.B. Alterations in virulence and antibiotic resistant genes of multidrug-resistant Salmonella serovars isolated from poultry: The bactericidal efficacy of Allium sativum. *Microb. Pathog.* **2017**, *108*, 91–100, https://doi.org/10.1016/j.micpath.2017.05.008.
40. Eloff, J.N. A sensitive and quick microplate method to determine the minimal inhibitory concentration of plant extracts for bacteria. *Planta Med.* **1998**, *64*, 711–713, https://doi.org/10.1055/s-2006-957563.
41. Dardeer, H.M.; Assran, A.S.; Al-Hussain, S.A.; Toghan, A. Synthesis, spectroscopic and molecular docking studies of novel 10-heterylazo-9-anthrone derivatives as potential antimicrobial and anticancer agents. *J. Mol. Struct.* **2021**, *1226*, 129359, https://doi.org/10.1016/j.molstruc.2020.129359.
42. Toghan, A.; Gadow, H.S.; Dardeer, H.M.; Elabbasy, H.M. New promising halogenated cyclic imides derivatives as potential corrosion inhibitors for carbon steel in hydrochloric acid solution. *J. Mol. Liq.* **2021**, *325*, 115136, https://doi.org/10.1016/j.molliq.2020.115136.
43. Appel, R.; Loos, R.; Mayr, H. Nucleophilicity parameters for phosphoryl-stabilized carbanions and phosphorus ylides: Implications for wittig and related olefination reactions. *J. Am. Chem. Soc.* **2009**, *131*, 704–714, https://doi.org/10.1021/ja8056216.
44. Byrne, P.A.; Gilheany, D.G. The modern interpretation of the wittig reaction mechanism. *Chem. Soc. Rev.* **2013**, *42*, 6670–6696, https://doi.org/10.1039/C3CS60105F.
45. Toghan, A.; Abo-Bakr, A.M.; Rageh, H.M.; Abd-Elsabour, M. Green electrochemical strategy for one-step synthesis of new catechol derivatives. *RSC Adv.* **2019**, *9*, 13145–13152, https://doi.org/10.1039/C9RA01206K.
46. Dardeer, H.M.; Taha, A.G.; Elamary, R.B. Synthesis, characterization, and antimicrobial evaluation of some novel anthracene heterocycles derivatives. *J. Heterocycl. Chem.* **2020**, *57*, 3951–3960, https://doi.org/10.1002/jhet.4104.
47. Samadpour, A.N.; Merrikh, H. DNA gyrase activity regulates DnaA-dependent replication initiation in Bacillus subtilis. *Mol. Microbiol.* **2018**, *108*, 115–127, https://doi.org/10.1111%2Fmmi.13920.

48. Tanitame, A.; Oyamada, Y.; Ofuji, K.; Fujimoto, M.; Iwai, N.; Hiyama, Y.; Suzuki, K.; Ito, H.; Terauchi, H.; Kawasaki, M.; Nagai, K.; Wachi, M.; Yamagishi, J.I. Synthesis and antibacterial activity of a novel series of potent DNA gyrase inhibitors. Pyrazole derivatives. *J. Med. Chem.* **2004**, *47*, 3693–3696, https://doi.org/10.1021/jm030394f.
49. Rashdan, H.R.M.; Shehadi, I.A.; Abdelmonsef, A.H. Synthesis, Anticancer Evaluation, Computer-Aided Docking Studies, and ADMET Prediction of 1,2,3-Triazolyl-Pyridine Hybrids as Human Aurora B Kinase Inhibitors. *ACS Omega* **2021**, *6*, 1445–1455, https://doi.org/10.1021/acsomega.0c05116.
50. Noser, A.A.; El-Naggar, M.; Donia, T.; Abdelmonsef, A.H. Synthesis, *In silico* and *In vitro* Assessment of New Quinazolinones as Anticancer Agents via Potential AKT Inhibition. *Molecules* **2020**, *25*, 4780, https://doi.org/10.3390/molecules25204780.
51. Noser, A.A.; Abdelmonsef, A.H.; El-Naggar, M.; Salem, M.M. New Amino Acid Schiff Bases as Anticancer Agents via Potential Mitochondrial Complex I-Associated Hexokinase Inhibition and Targeting AMP-Protein Kinases/mTOR Signaling Pathway. *Molecules* **2021**, *26*, 5332, https://doi.org/10.3390/molecules26175332.
52. Abo-Bakr, A.M.; Alsoghier, H.M.; Abdelmonsef, A.H. Molecular Docking, Modeling, Semiempirical Calculations Studies and *In vitro* Evaluation of New Synthesized Pyrimidin-imide Derivatives. *J. Mol. Struct.* **2022**, *1249*, 131548, https://doi.org/10.1016/j.molstruc.2021.131548.
53. Haredi Abdelmonsef, A.; Eldeeb Mohamed, M.; El-Naggar, M.; Temairk, H.; Mohamed Mosallam, A. Novel Quinazolin-2,4-Dione Hybrid Molecules as Possible Inhibitors Against Malaria: Synthesis and *in silico* Molecular Docking Studies. *Front. Mol. Biosci.* **2020**, *7*, 105, https://doi.org/10.3389/fmolb.2020.00105.
54. Gomha, S.M.; Abdelhady, H.A.; Hassain, D.Z.; Abdelmonsef, A.H.; El-Naggar, M.; Elaasser, M.M.; Mahmoud, H.K. Thiazole-Based Thiosemicarbazones : Synthesis, Cytotoxicity Evaluation and Molecular Docking Study. *Drug Des. Devel. Ther.* **2021**, *2021*, 659–677, https://doi.org/10.2147/DDDT.S291579.
55. Lipinski, C.A.; Lombardo, F.; Dominy, B.W.; Feeney, P.J. Experimental and Computational Approaches to Estimate Solubility and Permeability in Drug Discovery and Develop ment Settings. *Adv. Drug Deliv. Rev.* **2001**, *46*, 3–26, https://doi.org/10.1016/S0169-409X(00)00129-0.